Published in final edited form as:
Acta Biomater. 2012 February ; 8(2): 559–569. doi:10.1016/j.actbio.2011.10.003.

Modular Polymer Design to Regulate Phenotype and Oxidative Response of Human Coronary Artery Cells for Potential Stent Coating Applications

Spencer W. Crowder, **Mukesh K. Gupta**, **Lucas H. Hofmeister**, **Angela L. Zachman**, and **Hak-Joon Sung***
Department of Biomedical Engineering, Vanderbilt University, Nashville, TN, USA

Abstract

Polymer properties can be tailored by copolymerizing subunits with specific physicochemical characteristics. Vascular stent materials require biocompatibility, mechanical strength, and prevention of restenosis. Here we copolymerized poly(ε-caprolactone) (PCL), poly(ethylene glycol) (PEG), and carboxyl-PCL (cPCL) at varying molar ratios and characterized the resulting material properties. We then performed a short-term evaluation of these polymers for their applicability as potential coronary stent coating materials with two primary human coronary artery cell types: smooth muscle cells (HCASMCs) and endothelial cells (HCAECs). Changes in proliferation and phenotype were dependent upon intracellular reactive oxygen species (ROS) levels, and 4%PEG-96%PCL-0%cPCL was identified as the most appropriate coating material for this application. After three days on this substrate, HCASMCs maintained a healthy contractile phenotype and HCAECs exhibited a physiologically-relevant proliferation rate and a balanced redox state. Other test substrates promoted a pathological, synthetic phenotype in HCASMCs and/or hyperproliferation in HCAECs. Phenotypic changes of HCASMCs appeared to be modulated by Young's modulus and surface charge of test substrates, indicating a structure-function relationship that can be exploited for intricate control over vascular cell functions. These data indicate that tailored copolymer properties can direct vascular cell behavior and provide insight for further development of biologically instructive stent coating materials.

Keywords

polycaprolactone; endothelial cell; smooth muscle cell; superoxide; hydrogen peroxide

1. Introduction

The physicochemical and mechanical properties of biomaterials modulate the response of the cells and tissues with which they interact [1–4]. In particular, polymers can be designed to control cell activity and fate through structure-function relationships [4]. Copolymerization techniques provide a means for tuning polymer properties by

*Corresponding author: Tel: +1 615 322 6986 Fax: +1 615 343 7919, hak-joon.sung@vanderbilt.edu (H-J Sung).
Present Address: Department of Biomedical Engineering, VU Station B #351631, 2301 Vanderbilt Place, Nashville, TN 37235 U.S.A.

The authors confirm that there are no known conflicts of interest.

incorporating subunits with different characteristics and varying their molar ratios, thereby controlling micro and macro structures [4]. By understanding the effect of each subunit on the resulting polymer properties, as well as the ability of each subunit to modulate a cellular response, polymer properties can be precisely optimized to control a specific biological function.

Implantation of a vascular stent is crucial to reduce human morbidity and mortality resulting from a vascular disease-induced, localized blood flow constriction [5]. Current stent technologies include bare metal stents, polymers, and drug eluting stents (e.g., bare metal stents with surface coating of polymers and drugs), yet each of these technologies poses a specific set of issues that has prevented its dominance of the clinical market. For example, bare metal stents are non-biodegradable and have been shown to cause restenosis; certain types of polymer stents can produce byproducts that stimulate an inflammatory response; and drug eluting stents promote late thrombosis resulting from delayed re-endothelialization [5, 6]. Therefore, much attention has recently been paid to design instructive, bioactive, and bioresorbable materials as a solution to problems associated with classical treatments [7]. The ideal properties of a stent material include sufficient mechanical strength, moderate degradation kinetics, resorbable byproducts, and regulation of cellular activities (i.e., proliferation, viability), each of which can be precisely controlled by understanding how polymer chemistry affects the subsequent cellular response.

In order to design polymers for potential coronary stent coating applications, insight into how these materials modulate the response of the cells with which they interact is of the utmost importance. The vasculature is primarily comprised of smooth muscle cells (SMCs) and endothelial cells (ECs). In general, healthy vascular SMCs proliferate at a very low rate and assume a contractile phenotype that is characterized by smooth muscle myosin heavy chain (smMHC) expression, and a spindle-like morphology [8, 9]. In contrast, unhealthy, “dedifferentiated” SMCs assume a circular, cobble stone-like synthetic phenotype in which smMHC expression is significantly down-regulated [8]. Understanding how polymer properties modulate SMC proliferation, growth, and phenotypic changes, as well as EC proliferation, is critical to designing a vascular stent coating that prevents restenosis. Maintenance of homeostatic redox balance differs in endothelial [10, 11] and smooth muscles cells [12]. Specifically, H_2O_2 has been shown to arrest proliferation in human coronary artery smooth muscle cells (HCASMCs) but promote proliferation in human coronary artery endothelial cells (HCAECs) [11–13]. Balance of cellular oxidative mechanisms is crucial for maintaining vascular homeostasis and preventing pathogenesis; aberrant ROS activities have been implicated in several cardiovascular diseases including hypertension and atherosclerosis [11–15]. Polymer composition has been shown to influence ROS activity [3, 4] and we therefore chose to focus on intracellular ROS levels to evaluate how oxidative activity is involved in the maintenance of healthy SMC and EC behavior.

In this study, we have developed a new class of copolymers with tunable mechanical and chemical properties for biomedical applications, specifically for potential coronary stent coating materials. Three subunits were copolymerized at varying molar ratios: poly(ε-caprolactone) (PCL) is a slow degrading, hydrophobic, highly biocompatible polymer that has been used in various biomedical applications [2, 16, 17]; poly(ethylene glycol) (PEG) is a hydrophilic polyether that can influence surface chemistry related to anti-adhesion of proteins and cells [18], bulk and degradation properties [19, 20] and oxidative activity [3, 4]; and, carboxyl PCL (cPCL) which carries a negative charge that improves hydrophilicity, can counteract repellent effects of PEG [4], and provides a site for functionalization of bioactive molecules to the polymer backbone [21]. A representative library of copolymers was synthesized and characterized, and thin film samples were prepared as culture substrates for primary HCASMCs and HCAECs as a short-term evaluation of the applicability of these

polymers for future use as a coronary stent coating material. We investigated changes in phenotype and cellular activities of HCASMCs and HCAECs which are related to reactive oxygen species (ROS)-mediated processes, as well as potential structure–function relationships between test materials and their ability to modulate cellular ROS activities. As a result, we identified the material properties that promoted vascular homeostasis, physiologically-relevant proliferation rates, and balanced redox activities for both cell types. This structure-function relationship provides an insight into effective methods for outside-in control of healthy vascular cell function and specific material properties to reduce the pathological response that has been problematic in coronary stent applications.

2. Materials and Methods

2.1 Polymer Synthesis and Test Substrate Preparation

Poly(ethylene glycol) (PEG, M_w = 5000) was purchased from Sigma Aldrich (St. Louis, MO). Poly(ε-caprolactone) (PCL) homopolymer as well as PEG, PCL, and carboxyl-PCL (cPCL) copolymers were synthesized according to methods previously described [21–23] (Fig.1A). PCL polymers were synthesized by ring-opening polymerization and, in the case of copolymers, were extended from PEG. Terpolymers (i.e., polymers containing all three subunits) were synthesized according to the method reported previously [21], but with x %PEG-*b*-y%PCL as the starting material. Copolymers of *x* mol % PEG, *y* mol % PCL, and *z* mol % cPCL were identified as *x*%PEG-*b*-*y%*PCL-*co*-*z*%cPCL where PEG-PCL is a block copolymer but cPCL addition is random within the PCL subunit. The polymers are abbreviated *x*%PEG-*y*%PCL-*z*%cPCL.

Polymer structure and molar percentages were confirmed by ^{1}H NMR spectra:
100%PCL: ^{1}H NMR ($CDCl_3$) = δ 4.06 (t, 3H, -OCH_2), 2.31(t, 2H, -CH_2), 1.66 (m, 2H, -CH_2), 1.37 (m, 4H, -CH_2) ppm; **90%PCL-10%cPCL:** ^{1}H NMR ($CDCl_3$) = δ 4.06 (t, 3H, -OCH_2), 3.4 (m, 1H, -CH-COOH), 2.31(t, 2H, -CH_2), 1.66 (m, 2H, -CH_2), 1.37 (m, 2H, -CH_2) ppm; **4%PEG-96%PCL:** ^{1}H NMR ($CDCl_3$) = δ 4.06 (t, 3H, -OCH_2), 3.65 (s, 4H, -OCH_2), 2.31(t, 2H, -CH_2), 1.66 (m, 2H, -CH_2), 1.37 (m, 4H, -CH_2) ppm;
8%PEG-92%PCL: ^{1}H NMR ($CDCl_3$) = δ 4.06 (t, 3H, -OCH_2), 3.65 (s, 4H, -OCH_2), 2.31(t, 2H, -CH_2), 1.66 (m, 2H, -CH_2), 1.37 (m, 4H, -CH_2) ppm;
4%PEG-86%PCL-10%cPCL: ^{1}H NMR ($CDCl_3$) = δ 4.06 (t, 3H, -OCH_2), 3.4 (m, 1H, -CH-COOH), 2.31(t, 2H, -CH_2), 1.66 (m, 2H, -CH_2), 1.37 (m, 2H, -CH_2) ppm;
8%PEG-82%PCL-10%CPCL: ^{1}H NMR ($CDCl_3$) = δ 4.06 (t, 3H, -OCH_2), 3.4 (m, 1H, -CH-COOH), 2.31(t, 2H, -CH_2), 1.66 (m, 2H, -CH_2), 1.37 (m, 2H, -CH_2) ppm.

For testing mechanical and thermal properties, solvent cast films were prepared at 5% weight/volume (w/v) in dichloromethane in a 100mm glass Petri dish, left at room temperature in air overnight, and then placed under vacuum for two days to remove excess solvent. For biological experiments, cover glass samples were prepared by spin coating (WS-650SZ-6NPP/Lite Spin Coater, Laurell Technologies, North Wales, PA) at 1% w/v in 70/30 chloroform/dimethylformamide onto 15mm glass cover slips at 4,000 RPM for 30 seconds. Samples were placed under vacuum for at least two days before use to remove organic solvent completely. Samples for cellular interaction experiments were sterilized under UV light for 1 hour. Differences in sample preparation can be attributed to specific testing requirements. For example, mechanical testing requires a stand-alone film (solvent cast) whereas a thin film supported by an underlying glass substrate (spin coat) is most appropriate for cell culture applications.

2.2 Thermal and Mechanical Properties

Differential scanning calorimetry (DSC, Q1000, TA Instruments, New Castle, DE) was performed with sample mass between 5 and 10 mg in aluminum pans with tops. The procedure included two temperature sweeps from −80°C to 100°C with a ramp rate of 10°C / minute. The values from the second sweep were reported such that thermal history was erased (n = 3). Thermogravimetric analysis (TGA-1000, Instrument Specialist Inc., Twin Lakes, WI) was performed using a heating rate of 20°C / minute to a final temperature of 600°C. Dried polymer powder was used for DSC and TGA experiments.

Dynamic mechanical analysis (DMA, Q800 DMA, TA Instruments) was performed with samples that were soaked in dH_2O at 37°C for 2 days prior to testing. Samples were hydrated prior to testing to evaluate the mechanical properties as they would be in physiological conditions. Wet stress and strain were recorded using a submersion clamp containing dH_2O at room temperature. A preload force of 0.1 N was applied to each sample and force was increased at a rate of 0.1 N/minute until failure. The average Young's Modulus is reported (n = 3). For temperature sweeps, a tension clamp was used with dry samples in air. The procedure included two runs from −80°C to 50°C with a ramp rate of 20 °C/minute and a displacement of 30 μm at 1 Hz (original sample length was 25mm). All values were calculated using Universal Analysis software provided by TA Instruments.

2.3 Molecular Weight and Degradation

Gel permeation chromatography (GPC, Shimadzu Corp., Kyoto, Japan) with an inline light scattering detector (miniDAWN TREOS, Wyatt Technology Corp., Santa Barabara, CA) was used to measure M_n based upon dn/ dC for each polymer type (n = 4). Solvent cast film samples (as described in Section 2.1) were used for GPC experiments [24]. Polymer samples were dissolved in tetrahydrofuran (THF, Sigma) at 1% w/v and filtered (0.2 μm pore size, Whatman, Kent, United Kingdom). For degradation studies, the intact polymer films were lyophilized following incubation in PBS, dissolved in THF, and filtered for measurements. A sample volume of 10 μL from the filtered solution was injected for each measurement. Degradation properties of polymers were characterized by measuring M_n over time (i.e., 0, 4, 7, and 28 days after incubation of polymer samples in phosphate buffer saline (PBS) at 37 °C). Initial M_n values for all polymers ranged from 60 – 140 kDa (100%PCL – 94 kDa; 90%PCL-10%cPCL – 140 kDa; 4%PEG-96%PCL – 73 kDa; 8%PEG-92%PCL – 63 kDa; 4%PEG-86%PCL-10%cPCL – 96 kDa; 8%PEG-82%PCL-10%cPCL – 82 kDa).

2.4 Surface Chemical Properties

The sessile drop method was used to measure contact angle with an in-house goniometer [25]. One 10 μL drop of dH_2O was placed on each solvent-cast film, pictures were taken immediately, and the angles on both sides of the drop were measured to represent "dry" contact angles. Samples were then incubated with dH_2O drops for 2 hours at 37 °C and measurements were taken to represent "wet" contact angles. All contact angles were analyzed through imaging and image analysis using ImageJ software (National Institutes of Health, Bethesda, MD) (n = 3).

In order to characterize the negative surface charge created by the carboxyl groups of cPCL, polymer-coated cover glasses were incubated with 1% v/v carboxylate-terminated, fluorescence-conjugated polystyrene microspheres (Sigma) in water overnight at 37 °C. Carboxyl groups generate a negative charge on the microsphere surface and microspheres are therefore repelled more by the polymer surface as cPCL % increases. Test samples were gently washed three times to remove repelled microspheres from the test surfaces but not to dislodge bound microspheres. The fluorescence intensity of remaining microspheres on the test sample was then measured with a plate reader (infinite F500, Tecan Group Ltd.,

Mannedorf, Switzerland) at 575 nm and 610 nm excitation and emission wavelengths, respectively (n = 4). This method indirectly probes surface charge through charge repulsion of microspheres and allows for easy comparison between sample groups.

2.5 Cell Culture

HCASMCs (passages 6–8) were cultured in Dulbecco's Modified Eagle's Medium (DMEM, Gibco Cell Culture, Carlsbad, CA) supplemented with 10% heat-inactivated fetal bovine serum (FBS, Gibco), 1% penicillin-streptomycin (Gibco), and 1% L-glutamine (Gibco). HCASMCs were seeded at a density of 15,000 cells / well in a 24-well plate (~8,500 cells / cm^2). HCAECs (passage 7) were cultured in MesoEndo Growth Medium (Cell Applications, Inc., San Diego, CA) supplemented with 10% FBS and 1% penicillin-streptomycin. HCAECs were seeded at a density of 10,000 cells / well in a 24-well plate (~5,500 cells / cm^2). Cells were purchased from Cell Applications, Inc. (San Diego, CA). Cells were cultured for three days on test polymer samples before end point experiments in order to evaluate short-term response to polymer test substrates following the previous studies [3, 4].

2.6 Immunofluorescence Staining

To measure proliferation, cells were incubated with 5-bromo-2'-deoxyuridine (BrdU, Sigma) at 20 μM for 16 hours. For all staining experiments, cells were fixed in 4% paraformaldehyde (Sigma) in dH_2O and incubated with primary antibody (1:100) overnight at 4 °C. For proliferation experiments only, DNA was denatured by treatment with hydrochloric acid (2N for 12 minutes on ice, 1N for 20 minutes at 37°C) which was neutralized with borate buffer (pH 9.0). Incorporated BrdU in proliferating cells was detected by staining with rat anti-BrdU antibodies (1:100, Abcam, Cambridge, MA), followed by addition of secondary DyLight594-conjugated goat anti-rat antibodies (1:50, Jackson Immunoresearch, West Grove, PA). To evaluate a healthy contractile phenotype in HCASMCs, expression of smooth muscle myosin heavy chain (smMHC) was detected by staining with primary mouse anti-human smMHC antibodies (1:100, Abcam), followed by addition of secondary TRITC-conjugated goat anti-mouse (1:50, Abcam) antibodies. To evaluate inflammatory action of HCAECs, expression of vascular cell adhesion molecule (VCAM)-1 was detected by staining with APC-conjugated anti-human VCAM-1 antibodies (5 μg / mL, CD 106, BioLegend, San Diego, CA). Cells were incubated with lipopolysaccharide (LPS, 1 μg / mL, Sigma) for one day to stimulate VCAM expression and used as a positive control group [26, 27]. Cell nuclei were counterstained with Hoechst 33258 (5 μg / mL, Sigma) in all the aforementioned types of fluorescence staining. Cells were imaged under a Nikon Eclipse Ti inverted fluorescence microscope (Nikon Instruments Inc, Melville, NY). Protein expression was quantified as the fluorescence intensity from antibody staining experiments using ImageJ software. All fluorescence values were normalized to cell number by counting Hoechst-stained nuclei within a given region of interest. Normalized values were compared between groups and are presented as relative expression levels. Cell proliferation was represented by the percent of BrdU-positive cells relative to the total number of cells per image (%) (n = 12 images).

2.7 Cell Activities

HCASMCs or HCAECs were incubated with dihydroethidium (DHE, Invitrogen) and dichlorofluorescein diacetate (DCFDA, Invitrogen) for 30 minutes at 5 μg / mL to measure intracellular superoxide and hydrogen peroxide, respectively, following the previously reported method [4]. To measure cell viability, HCASMCs or HCAECs were stained with calcein AM (1 μg / mL, Invitrogen). All cells were counterstained with Hoechst nucleus staining (5 μg / mL) to measure the total number of cells. Fluorescence intensity of each staining (i.e., DHE, DCFDA, and calcein AM) was measured with a plate reader (Tecan) and were normalized to the corresponding cell number (excitation/emission: DHE 350/600,

DCFDA 490/540, Hoechst 360/488, calcein 495/515). To measure total protein content, cells were lysed and proteins were harvested and quantified by a colorimetric assay (BioRad, Hercules, CA). For morphological analysis, the actin cytoskeleton of HCASMCs was visualized with Texas Red-X phalloidin (Invitrogen) and cell circularity was measured using ImageJ (n = 80 cells from >3 images) [28]. Degree of circularity is a 0–10 scale defined as 0 being a line and 10 representing a perfect circle (circularity = 40π*(area/perimeter^2)). Therefore, cells with circularity closer to zero are considered to be more elongated whereas cells with circularity closer to ten are considered to be rounded. To ensure accurate measurements, at least half of the cells that were measured (>40 cells / polymer) were either not in contact with other cells or showed only minimal cell-cell contact.

2.8 Statistical Analysis

In all experiments, results are presented as mean ± standard error of the mean (SEM). Results from each experiment were initially analyzed using single factor analysis of variance and comparisons between individual sample groups were then performed using an unpaired Student's t-test. For all statistics, $p < 0.05$ was considered statistically significant.

3. Results

3.1 Synthesis

A subset of six polymers were synthesized, characterized and evaluated for cellular interaction: 100%PCL, 90%PCL-10%cPCL, 4%PEG-96%PCL, 8%PEG-92%PCL, 4%PEG-86%PCL-10%cPCL, and 8%PEG-82%PCL-10%cPCL (Fig. 1A).

3.2 Degradation

M_n was measured by GPC following incubation of each polymer sample in PBS at 37 °C at the indicated time points over 28 days. The M_n of 100%PCL decreased by ~13% at 28 days post incubation (Fig. 1B). With the addition of 10%cPCL to the PCL homopolymer (i.e., 90%PCL-10%cPCL), the polymer degraded more quickly (~19%) and this effect was enhanced (~25%) upon addition of the hydrophilic 4% PEG subunit (i.e. 4%PEG-90%PCL-10%cPCL). These polymers were selected as representative samples to demonstrate how each subunit affects degradation properties.

3.3 Thermal Properties

Thermal degradation of each polymer sample was first evaluated by TGA. The results reveal stability of all polymers up to 200 °C, supporting their use in physiological applications at 37°C (Fig. 2A). DSC was then used to monitor changes in the thermal properties of different polymer compositions (Fig. 2B). The enthalpy change (ΔH) and melting temperature (T_m) of 100%PEG was higher than those of 100%PCL. Compared to 100%PCL, ΔH increased slightly upon addition of PEG to the PCL homopolymer (i.e., 4%PEG-96%PCL and 8%PEG-92%PCL), but decreased with cPCL (i.e., 90%PCL-10%cPCL) (Fig. 2B). Interestingly, addition of both PEG and cPCL in the terpolymers (i.e., 4%PEG-86%PCL-10%cPCL and 8%PEG-82%PCL-10%cPCL) greatly decreased ΔH, compared to the test homo- and copolymers. Also, ΔH increased as the PEG content increased from 4% to 8% in the test terpolymers. The DMA results showed that the wet glass transition temperature (Wet T_g) decreased as the PEG and/or the cPCL content(s) increased in the test polymer types (Table 1). In particular, in the test terpolymers, the addition of cPCL amplified the PEG effect, resulting in a further reduction of wet T_g.

3.4 Wet Mechanical Properties

DMA was used to evaluate the wet mechanical properties of the test polymers. Upon addition of cPCL (i.e., 90%PCL-10%cPCL), the wet Young's modulus (E) and ultimate tensile strength (σ_U) decreased, compared to 100%PCL (Table 1). Addition of PEG (i.e., 4%PEG-96%PCL and 8%PEG-92%PCL) also decreased these parameters compared to 100%PCL, but to a lesser extent than 90%PCL-10%cPCL. In terpolymers, addition of both PEG and cPCL dramatically reduced E and σ_U, compared to the test homo- and copolymers, indicating the combined effects of PEG and cPCL on the mechanical properties.

3.5 Water Contact Angle and Surface Charge

Using the sessile drop method, water contact angle was assessed to evaluate the ability of PEG and cPCL subunits to modulate surface hydrophilicity (Fig. 3A). The sessile contact angle at 0 hours was not significantly different among the test polymer types. Following incubation for 2 hours at 37 °C with 95% humidity, contact angles decreased significantly in PEG- and/or cPCL-containing polymers due to water absorption. In particular, the contact angle at 2 hours decreased as the cPCL and/or PEG content increased in the test polymer types, indicating the contributions of the PEG and cPCL hydrophilic subunits. The contact angles at 2 hours were less than 10° on the test terpolymers, indicating that the test surfaces fully absorbed the drop.

Relative negative surface charge was evaluated by employing the concept of charge-charge repulsion between free carboxyl groups on microspheres and the polymer surface. Strong fluorescence intensity indicates a surface with less negative charge due to reduced charge-charge repulsion. The relative fluorescence intensity of polymer-coated cover glass was measured following overnight incubation with carboxylate-terminated fluorescent microspheres (Fig. 3B). The 100%PCL surface exhibited the highest fluorescence intensity, indicating the least negative charge. The addition of cPCL reduced the fluorescence intensity significantly, as compared to the test polymers that do not contain cPCL, suggesting the presence of negative surface charge derived from cPCL. The lowest fluorescence intensities were observed for the test terpolymers, indicating an additional repellent effect of PEG in combination with cPCL. As a control, we used tissue culture polystyrene wells, which are negatively charged and therefore repelled almost all microspheres, supporting the conceptual approach of this technique.

3.6 Cellular Interaction

3.6.1 HCASMC Response—To determine the optimal chemistry of polymers for potential coronary stent coating applications, responses of HCASMCs to test polymers were first investigated. After three days of culture, we measured intracellular reactive oxygen species (ROS) levels, specifically superoxide ($O_2^{\bullet-}$) and hydrogen peroxide (H_2O_2), and found them to vary significantly between test polymer types (Fig. 4A–B). Intracellular $O_2^{\bullet-}$ levels correlated inversely with intracellular H_2O_2 levels except in the case of 4%PEG-96%PCL (Fig. 4A). For example, 8%PEG-92%PCL displayed a low level of $O_2^{\bullet-}$, but a high level of H_2O_2; conversely, test terpolymers displayed the highest levels of $O_2^{\bullet-}$ and the lowest levels of H_2O_2. In the test co- and terpolymers, increasing PEG molar ratios resulted in higher intracellular H_2O_2 levels, but this effect was counteracted by the addition of negatively-charged cPCL (Fig. 4B). HCASMCs grown on terpolymers displayed higher $O_2^{\bullet-}$ levels and lower H_2O_2 levels relative to test copolymers ($p < 0.05$ between individual test polymers).

HCAMSCs in all polymer groups maintained viability (> 70%), but proliferation varied significantly (Fig. 4C–D). Percentages of proliferating HCASMCs correlated proportionally with total protein content for each group (Fig. 4d–e). HCAMSCs grown on terpolymers

resulted in significantly higher values for proliferation and total protein content relative to copolymers ($p < 0.05$ between individual test polymers). Interestingly, proliferation correlated inversely with intracellular H_2O_2 levels except in the case of 100%PCL (Fig. 4A).

In order to test the ability of the different polymers to discourage a pathogenic, synthetic phenotype, we stained for smMHC and found that 4%PEG-96%PCL promoted a statistically greater level of smMHC expression in HCASMCs relative to all other conditions ($p < 0.01$, Fig. 4F). Additionally, HCASMCs morphology was altered depending upon substrate composition (Fig. 5). Degree of circularity is a 0–10 scale in which values closer to zero represent a more elongated morphology and 10 represents a perfect circle. 100%PCL and 90%PCL-10%cPCL showed a slight trend towards a less circular morphology distribution. 4%PEG-96%PCL showed the most distinct peak for a low degree of circularity with smallest standard deviation (standard deviation, SD = 1.31) of all groups, supporting the highest smMHC expression of HCASMCs on this polymer. In contrast, 8%PEG-92%PCL showed the most distinct peak at a high degree of circularity. Interestingly, the test substrates containing PEG without cPCL resulted in the two strongest morphological biases (e.g. towards elongated morphology for 4%PEG-96%PCL and slightly more rounded for 8%PEG-92%PCL)of all polymers tested, likely due to the ability of PEG to modulate protein adsorption and cell adhesion [3]. The terpolymers showed bimodal circularity distributions that represent the contributions from all three polymeric subunits: 100%PCL promotes slightly elongated morphologies, 90%PCL-10%cPCL promotes an even distribution of centered morphologies (degree of circularity ~5), and PEG-containing copolymers bias the cell morphology towards elongated or rounded, depending upon molar percentage (Fig. 5).

3.6.2 HCAECs Response—We then evaluated the responses of HCAECs to test polymer substrates. We found that trends in ROS levels of HCAECs were opposite to those of HCASMCs (Fig. 6A). HCAECs on the 8%PEG- 92%PCL copolymer exhibited a statistically higher level of $O2^{\bullet-}$ expression relative to all other groups except 4%PEG-96%PCL ($p < 0.01$ between individual test polymers, Fig. 6A). Intracellular H_2O_2 levels of HCAECs correlated inversely with $O2^{\bullet-}$(Fig. 6B), which was similar to the trends seen in HCASMCs (Fig. 4A and B). HCAECs proliferation was high (> 50%) in all groups except 4%PEG-96%PCL (20–30%), which was significantly lower than 100%PCL ($p < 0.01$) and all other groups ($p < 0.05$, Fig. 6C). To evaluate if any of the polymers stimulate pro-inflammatory activation of HCAECs, VCAM-1 expression of HCAECs was measured on test polymers. The condition with lipopolysaccharide (LPS) treatment was used as a positive control (Fig. 6D) [26, 27]. VCAM-1 expression in ECs is stimulated by pathological cues, resulting in recruitment of inflammatory cells, but its expression is extremely low in inactivated ECs [29]. We found that none of the polymers stimulated significant VCAM-1 expression compared to LPS-treated HCAECs, thereby further supporting the applicability of these polymers as biocompatible cardiovascular biomaterials, in particular for vascular stent coating applications (Fig. 6D).

4. Discussion

The purpose of this study was to synthesize and characterize a new class of copolymers with tunable mechanical and physicochemical properties for biomedical applications, particularly as potential coatings for coronary artery stents. Three subunits were co-polymerized at varying molar ratios: poly(ε-caprolactone) (PCL) was used as the primary component due to its biocompatibility, hydrophobicity, and slow degradation rate [2, 16, 17, 24]; poly(ethylene glycol) (PEG) to promote hydrophilicity, water absorption and to modulate repulsion of proteins and cells [4]; and carboxyl-PCL (cPCL) for increased hydrophilicity and exposure of a negative surface charge that was found to reduce the repellent effect of PEG [4, 21].

The three subunits exhibit distinct characteristics and, when copolymerized at different molar ratios, the resulting polymer can be tailored to modulate cellular response. The molar percentages chosen for PEG (e.g. 4% and 8%) are based upon findings from previous investigations that have revealed these percentages to be increasingly cell-repellent [3]. Investigations with two primary human vascular cell types revealed the structure-function relationships that control cell proliferation and phenotypic changes in a reactive-oxygen species (ROS)-dependent manner.

PCL is a semi-crystalline, hydrophobic polymer with slow degradation kinetics in aqueous environments [16, 17]. Addition of the random hydrophilic cPCL subunit or PEG block improved water absorption, facilitated hydrolytic cleavage, and resulted in a faster degradation rate (Fig. 1B). In dry conditions, adding cPCL reduced enthalpy change and melting temperature, most likely due to decreased chain regularity and crystallinity (Fig. 2B). Inclusion of the PEG block, however, increased these values. It is hypothesized that this is due to improved chain packing and crystallinity, which is supported by the values for 100%PEG. In wet conditions, addition of either cPCL or PEG reduced T_g, E, and σ_U (Table 1). This effect was further enhanced in the test terpolymers due to the increased water absorption by the hydrophilic subunits, which decreased crystallinity and reduced mechanical properties.

Polymer surfaces composed of increasing molar ratios of PEG and cPCL proportionally absorbed more water, as seen by contact angle analysis following 2 hours of incubation (Fig. 3A). The contact angle measurements at 0 hours do not reflect the hydrophilicity of the surface in physiological conditions, as these measurements were made immediately after introducing the water drop and culture conditions expose the surface to an aqueous environment indefinitely. For example, 4%PEG-96%PCL and 8%PEG-92%PCL copolymers exhibited a higher contact angle at 0 hours than 100%PCL. This counterintuitive result can likely be explained by progressive formation of segregated hydrophilic phase domains of PEG or cPCL [2]. As hydration increases over time, hydrophobic PCL and hydrophilic PEG or cPCL-containing surfaces rearrange dynamically to reach phase-separated micro to nanostructures that minimize free energy between surface-liquid interfaces. This potential of phase separation into PEG or cPCL-rich regions might have further enhanced hydration (“feedback mechanism”), resulting in the decreased water contact angle. Finally, incubation with carboxylate-terminated microspheres suggested differences in the surface characteristics between test polymer types ($p < 0.05$ vs. 100%PCL) (Fig. 3B). Tissue culture polystyrene wells have a negatively-charged, hydrophilic surface [30, 31] and demonstrated virtually no fluorescence signal, thereby supporting the concept of this technique. Differences in microsphere adherence to the test polymer surfaces might be explained by properties of the individual polymer subunits. 4%PEG-96%PCL and 8%PEG-92%PCL exhibited large deviations in surface fluorescence that were likely caused by phase separated domains that form at the polymer surface based upon differences in the properties of the polymer subunits [4]. Hydrophilic PEG domains likely repelled the spheres by favoring interactions with water and sterically hindering microsphere binding as opposed to hydrophobic PCL domains. In parallel, the lower fluorescence signal exhibited by cPCL-containing substrates, as compared to PCL and PEG-PCL substrates, suggests that the microspheres are repelled by the exposed, negative surface charge from cPCL. In terpolymer substrates specifically, the additive microsphere-repellent effects from both PEG and cPCL domains resulted in the lowest fluorescence signal of all test substrates. 100%PCL substrates, however, demonstrated the highest fluorescence signal, likely due to the hydrophobic surface of PCL that does not exhibit repellent effects from either water absorption or charge repulsion domains.

Homeostasis of vascular SMCs (VSMCs) and endothelial cells (VECs) is dependent upon effective redox mechanisms [8]. Imbalances in ROS, such H_2O_2 and $O_2^{\bullet-}$, result in abnormal cell proliferation, changes in phenotype, and the progression of cardiovascular diseases, including hypertension, atherosclerosis, and restenosis [13, 15, 32, 33]. VSMCs and VECs produce ROS at a basal level that is crucial for cell signaling. However, excess ROS, either from intracellular production or those released by inflammatory cells in pathological states, have been implicated in disease progression, specifically causing the "dedifferentiation" of VSMCs [8] and hyperproliferation of VECs [11]. Interestingly, H_2O_2 and $O_2^{\bullet-}$ have been shown to stimulate opposite responses in VSMCs and VECs: VSMCs proliferation is promoted by $O_2^{\bullet-}$ and arrested by H_2O_2 [12], but VECs proliferation is stimulated by H_2O_2 and arrested by $O_2^{\bullet-}$ [10, 11]. Healthy VSMCs are differentiated, quiescent, and maintain a contractile phenotype, which is characterized by an elongated spindle-like morphology and expression of smMHC [8, 14]. However, unhealthy VSMCs dedifferentiate, proliferate, assume a synthetic phenotype, a circular morphology, and display low smMHC expression. Healthy VECs proliferate slowly *in vivo* and hyperproliferation of VECs can lead to vessel blockage [10, 34]. These competitive signaling events reveal a complex framework in which maintenance of two healthy cell types requires a specific ROS balance. We therefore investigated the role of these polymers in modulating intracellular ROS production, cell proliferation, and phenotypic changes in HCASMCs and HCAECs, and identified structure-function relationships that provide healthy versus pathological environments.

As seen in Figure 4, HCASMCs intracellular ROS varied dramatically in response to different polymer substrates. In most groups, a high level of $O_2^{\bullet-}$ correlated with a low level of H_2O_2, suggesting the activity of superoxide dismutase (SOD) in converting $O_2^{\bullet-}$ to H_2O_2 [10, 11]. PEG-containing substrates have been shown to promote intracellular H_2O_2 production, as seen for HCASMCs cultured on 4%PEG-96%PCL and 8%PEG-92%PCL (Fig. 4B) [3, 4]. On the test terpolymers, the addition of cPCL counteracted the effects of PEG and resulted in the lowest H_2O_2 levels. Although HCASMCs on all polymers remained viable (Fig. 4C), differences in proliferation rates and total protein content reflect the ability of $O_2^{\bullet-}$ and H_2O_2 to promote and arrest HCASMCs proliferation, respectively (Fig. 1D–E). In most groups, increasing levels of H_2O_2 corresponded with decreased proliferation rate and protein content whereas increasing $O_2^{\bullet-}$ levels correlated with increased proliferation. However, HCASMCs on 100%PCL showed high intracellular H_2O_2 and low intracellular $O_2^{\bullet-}$, yet maintained a high proliferation rate and protein content. Because this is the only purely hydrophobic substrate, we believe that the cell-adhesive surface of hydrophobic 100%PCL promoted proliferation of this mesenchymal cell type and that this effect was more influential than the competing ROS-induced arrest of proliferation [2].

Expression of smMHC was statistically higher in HCASMCs grown on 4%PEG-96%PCL relative to all other groups (Fig. 4F). Morphological analysis revealed that cells on 4%PEG-96%PCL showed the strongest bias towards an elongated spindle-like morphology, which is a typical phenotype of healthy HCASMCs (Fig. 5). Interestingly, in these cells, both intracellular ROS types stayed within a moderate range that, along with strong smMHC expression, suggests an effective redox balance that maintained a healthy contractile phenotype. In contrast, cells grown on the test terpolymers displayed high levels of intracellular $O_2^{\bullet-}$, coupled with sustained proliferation rates and the lowest levels of smMHC expression in HCASMCs. Cell circularity of HCASMCs on the test terpolymers assumed a bimodal distribution, suggesting a heterogeneous population of contractile and synthetic phenotypes on these surfaces (Fig. 5). HCAMSCs on 8%PEG-92%PCL had high intracellular H_2O_2 and reduced proliferation, but low protein content (Fig. 4B–D), indicating that the repellent effect of PEG prevented cell attachment and cell-matrix interaction. Together these results indicate that 4%PEG-96%PCL is the most appropriate substrate to

maintain a healthy HCASMCs phenotype, as characterized by strong smMHC expression, a low proliferation rate, and an effective redox balance.

We then assessed the response of HCAECs on polymer substrates in order to understand how each polymer subunit can influence the two cell types differently. By monitoring the response of two complementary coronary artery cell types, we sought to identify the most appropriate polymer(s) for a coronary stent coating application. We found that trends in intracellular ROS levels of HCAECs were opposite to those of HCASMCs with respect to the substrate composition (Fig. 6A–B). Intracellular H_2O_2 was minimized on 4%PEG-96%PCL and 8%PEG-92%PCL whereas intracellular $O_2^{\bullet-}$ was increased. HCAECs on the test terpolymers displayed high levels of $O_2^{\bullet-}$ and low levels of H_2O_2. Proliferation rates agreed with intracellular ROS patterns except for HCAECs on 8%PEG-92%PCL, which displayed high intracellular $O_2^{\bullet-}$ and low H_2O_2, but maintained a high proliferation rate (~65%). As with HCASMCs, the 8%PEG-92%PCL exhibited a strong repellent effect that prevented cell-matrix interactions, but for HCAECs, the dominant cell-cell interactions promoted proliferation in an ROS-independent manner. HCAECs grown on all polymers except 4%PEG-96%PCL showed proliferation rates in a pathophysiological range (>40%), making them less ideal for cardiovascular application [32]. Finally, VCAM-1 expression, which is extremely low in inactivated ECs but strongly upregulated following activation, was barely detectable in HCAECs grown on polymer substrates. Although there is a low level of detectable VCAM-1 expression for HCAECs cultured on polymer substrates, it is not within the same order of magnitude as LPS-treated control. In comparison to the LPS-treated positive control, these findings demonstrate that none of the test substrates stimulate a significant inflammatory response in HCAECs. Taken together, these findings reveal that 4%PEG-96%PCL is the most appropriate material to promote healthy HCAEC activity, as seen by an intermediate production of intracellular ROS, maintenance of a physiologically-relevant proliferation rate, and absence of inflammatory stimulation when cultured on this substrate.

Polymer substrates were shown to modulate cellular activity in an ROS-mediated manner. Analysis of the relationships between polymer properties and the subsequent cellular response revealed structure-function relationships that may provide insight into manipulating cellular activities by exploiting specific polymer characteristics. Intracellular H_2O_2 in HCASMCs followed the same trend as the polymer mechanical properties (e.g. E and σ_U) whereas intracellular $O_2^{\bullet-}$ followed the same trend as the surface charge (inverse pattern from Fig. 3B). We believe that increased surface charge stimulates outside-in production of $O_2^{\bullet-}$, resulting in an abundance of intracellular $O_2^{\bullet-}$. Because intracellular $O_2^{\bullet-}$ promotes HCASMCs proliferation and HCASMCs are normally quiescent, more compliant substrates likely resemble a pathophysiological environment resulting from outward vascular remodeling that promotes proliferation, such as that found in atherosclerosis [35, 36]. For interactions with HCASMCs, 4%PEG-96%PCL was the best substrate because of its moderate surface charge and mechanical properties, as well as promotion of a balanced ROS production. This combination of properties promoted a healthy, contractile phenotype. Cellular behavior can also be modulated by the amount of PEG domains located at the polymer surface, such as with 8%PEG-92%PCL. HCASMCs, which are from the mesenchymal lineage, are cell-matrix interactive and did not grow well on this substrate; however, HCAECs, which are from the endothelial lineage, are cell-cell interactive and flourished. These responses did not follow the trends for cells on other test substrates and therefore provide interesting insight into control of competitive cell-cell versus cell-matrix interactions.

5. Conclusion

In this study, we have synthesized and characterized a new class of copolymers with tunable properties for biomedical applications. Polymer properties are influenced by the molar ratios of the individual subunits and, by varying their specific contributions, the resulting bulk and surface properties can be controlled. Investigation of the responses of two primary human coronary artery cell types revealed an ability of the substrate to modulate intracellular reactive oxygen species, which directed changes in phenotype and related cellular activities of the test cell types. Our study indicates that the polymer composition-dependent material properties can directly influence cellular response, in this case through ROS-mediated proliferation and phenotypic changes. Our findings suggest that materials with minimal surface charge and moderate stiffness (e.g. ~150 MPa) promote the healthiest response of primary coronary artery cells. Therefore, by expanding our class of polymers, we will validate the structure-function relationship and develop new methods to control cell behavior and health by modulating outside-in cell signaling.

Acknowledgments

Funding was provided by NIH grant HL091465 and NSF grant 1006558.

References

1. Lutolf MP, Hubbell JA. Synthetic biomaterials as instructive extracellular microenvironments for morphogenesis in tissue engineering. Nat Biotechnol. 2005; 23:47–55. [PubMed: 15637621]
2. Sung HJ, Su J, Berglund JD, Russ BV, Meredith JC, Galis ZS. The use of temperature-composition combinatorial libraries to study the effects of biodegradable polymer blend surfaces on vascular cells. Biomaterials. 2005; 26:4557–4567. [PubMed: 15722125]
3. Sung HJ, Chandra P, Treiser MD, Liu E, Iovine CP, Moghe PV, et al. Synthetic polymeric substrates as potent pro-oxidant versus anti-oxidant regulators of cytoskeletal remodeling and cell apoptosis. J Cell Physiol. 2009; 218:549–557. [PubMed: 19016472]
4. Sung H-J, Luk A, Murthy S, Liu E, Jois M, Joy A, et al. Poly(ethylene glycol) as a sensitive regulator of cell survival fate on polymeric biomaterials: the interplay of cell adhesion and pro-oxidant signaling mechanisms. Soft Matter. 2010; 6:5196–5205.
5. Mani G, Feldman MD, Patel D, Agrawal CM. Coronary stents: A materials perspective. Biomaterials. 2007; 28:1689–1710. [PubMed: 17188349]
6. Finn AV, Nakazawa G, Joner M, Kolodgie FD, Mont EK, Gold HK, et al. Vascular responses to drug eluting stents - Importance of delayed healing. Arteriosclerosis Thrombosis and Vascular Biology. 2007; 27:1500–1510.
7. Onuma Y, Ormiston J, Serruys PW. Bioresorbable Scaffold Technologies. Circulation Journal. 2011; 75:509–520. [PubMed: 21301138]
8. Su B, Mitra S, Gregg H, Flavahan S, Chotani MA, Clark KR, et al. Redox regulation of vascular smooth muscle cell differentiation. Circ Res. 2001; 89:39–46. [PubMed: 11440976]
9. Rovner AS, Murphy RA, Owens GK. Expression of smooth muscle and nonmuscle myosin heavy chains in cultured vascular smooth muscle cells. J Biol Chem. 1986; 261:14740–14745. [PubMed: 3533925]
10. Zanetti M, Zwacka R, Engelhardt J, Katusic Z, O'Brien T. Superoxide anions and endothelial cell proliferation in normoglycemia and hyperglycemia. Arterioscler Thromb Vasc Biol. 2001; 21:195–200. [PubMed: 11156852]
11. Cai H. Hydrogen peroxide regulation of endothelial function: origins, mechanisms, and consequences. Cardiovasc Res. 2005; 68:26–36. [PubMed: 16009356]
12. Li PF, Dietz R, vonHarsdorf R. Differential effect of hydrogen peroxide and superoxide anion on apoptosis and proliferation of vascular smooth muscle cells. Circulation. 1997; 96:3602–3609. [PubMed: 9396461]

13. Cai H, Harrison DG. Endothelial dysfunction in cardiovascular diseases: the role of oxidant stress. Circ Res. 2000; 87:840–844. [PubMed: 11073878]
14. Clempus RE, Griendling KK. Reactive oxygen species signaling in vascular smooth muscle cells. Cardiovasc Res. 2006; 71:216–225. [PubMed: 16616906]
15. Elahi MM, Kong YX, Matata BM. Oxidative stress as a mediator of cardiovascular disease. Oxid Med Cell Longev. 2009; 2:259–269. [PubMed: 20716913]
16. Zhang LL, Xiong CD, Deng XM. Biodegradable polyester blends for biomedical application. J Appl Pol Sci. 1995; 56:103–122.
17. Tang ZG, Black RA, Curran JM, Hunt JA, Rhodes NP, Williams DF. Surface properties and biocompatibility of solvent-cast poly[-caprolactone] films. Biomaterials. 2004; 25:4741–4748. [PubMed: 15120520]
18. Bergstrom K, Holmberg K, Safranj A, Hoffman AS, Edgell MJ, Kozlowski A, et al. Reduction of fibrinogen adsorption on PEG-coated polystyrene surfaces. J Biomed Mater Res. 1992; 26:779–790. [PubMed: 1527100]
19. Deschamps AA, van Apeldoorn AA, Hayen H, de Bruijn JD, Karst U, Grijpma DW, et al. In vivo and in vitro degradation of poly(ether ester) block copolymers based on poly(ethylene glycol) and poly(butylene terephthalate). Biomaterials. 2004; 25:247–258. [PubMed: 14585712]
20. Sun G, Zhang XZ, Chu CC. Effect of the molecular weight of polyethylene glycol (PEG) on the properties of chitosan-PEG-poly(N-isopropylacrylamide) hydrogels. J Mater Sci Mater Med. 2008; 19:2865–2872. [PubMed: 18347954]
21. Gimenez S, Ponsart S, Coudane J, Vert M. Synthesis, properties and in vitro degradation of carboxyl-bearing PCL. Journal of Bioactive and Compatible Polymers. 2001; 16:32–46.
22. Dong CM, Qiu KY, Cu ZW, Feng XD. Synthesis of star-shaped poly(epsilon-caprolactone)-b-poly(DL-lactic acid-alt-glycolic acid) with multifunctional initiator and stannous octoate catalyst. Macromolecules. 2001; 34:4691–4696.
23. Sosnik A, Cohn D. Poly(ethylene glycol)-poly(epsilon-caprolactone) block oligomers as injectable materials. Polymer. 2003; 44:7033–7042.
24. Sung HJ, Meredith C, Johnson C, Galis ZS. The effect of scaffold degradation rate on three-dimensional cell growth and angiogenesis. Biomaterials. 2004; 25:5735–5742. [PubMed: 15147819]
25. Kwok DY, Gietzelt T, Grundke K, Jacobasch HJ, Neumann AW. Contact angle measurements and contact angle interpretation .1. Contact angle measurements by axisymmetric drop shape analysis and a goniometer sessile drop technique. Langmuir. 1997; 13:2880–2894.
26. Dunzendorfer S, Lee HK, Soldau K, Tobias PS. Toll-like receptor 4 functions intracellularly in human coronary artery endothelial cells: roles of LBP and sCD14 in mediating LPS responses. FASEB J. 2004; 18:1117–1119. [PubMed: 15132988]
27. Zeuke S, Ulmer AJ, Kusumoto S, Katus HA, Heine H. TLR4-mediated inflammatory activation of human coronary artery endothelial cells by LPS. Cardiovasc Res. 2002; 56:126–134. [PubMed: 12237173]
28. Sung HJ, Eskin SG, Sakurai Y, Yee A, Kataoka N, McIntire LV. Oxidative stress produced with cell migration increases synthetic phenotype of vascular smooth muscle cells. Ann Biomed Eng. 2005; 33:1546–1554. [PubMed: 16341922]
29. Galkina E, Ley K. Vascular adhesion molecules in atherosclerosis. Arterioscler Thromb Vasc Biol. 2007; 27:2292–2301. [PubMed: 17673705]
30. Park JW, Roy D, Kwak JW, Maeng WJ, Kim H. Dendron-Modified Polystyrene Microtiter Plate: Surface Characterization with Picoforce AFM and Influence of Spacing between Immobilized Amyloid Beta Proteins. Langmuir. 2008; 24:14296–14305. [PubMed: 19053650]
31. O'Gara JP, Kennedy CA. Contribution of culture media and chemical properties of polystyrene tissue culture plates to biofilm development by Staphylococcus aureus. J Med Microbiol. 2004; 53:1171–1173. [PubMed: 15496399]
32. Hashimoto Y, Yoshinoya S, Aikawa T, Mitamura T, Miyoshi Y, Muranaka M, et al. Enhanced endothelial cell proliferation in acute Kawasaki disease (muco-cutaneous lymph node syndrome). Pediatric Research. 1986; 20:943–946. [PubMed: 3534782]

33. Newby AC, Zaltsman AB. Molecular mechanisms in intimal hyperplasia. J Pathol. 2000; 190:300–309. [PubMed: 10685064]

34. Meurice T, Vallet B, Bauters C, Dupuis B, Lablanche JM, Bertrand ME. Role of endothelial cells in restenosis after coronary angioplasty. Fundam Clin Pharmacol. 1996; 10:234–242. [PubMed: 8836697]

35. Tajaddini A, Kilpatrick DL, Vince DG. A novel experimental method to estimate stress-strain behavior of intact coronary arteries using intravascular ultrasound (IVUS). J Biomech Eng. 2003; 125:120–123. [PubMed: 12661205]

36. Khatri JJ, Johnson C, Magid R, Lessner SM, Laude KM, Dikalov SI, et al. Vascular oxidant stress enhances progression and angiogenesis of experimental atheroma. Circulation. 2004; 109:520–525. [PubMed: 14744973]

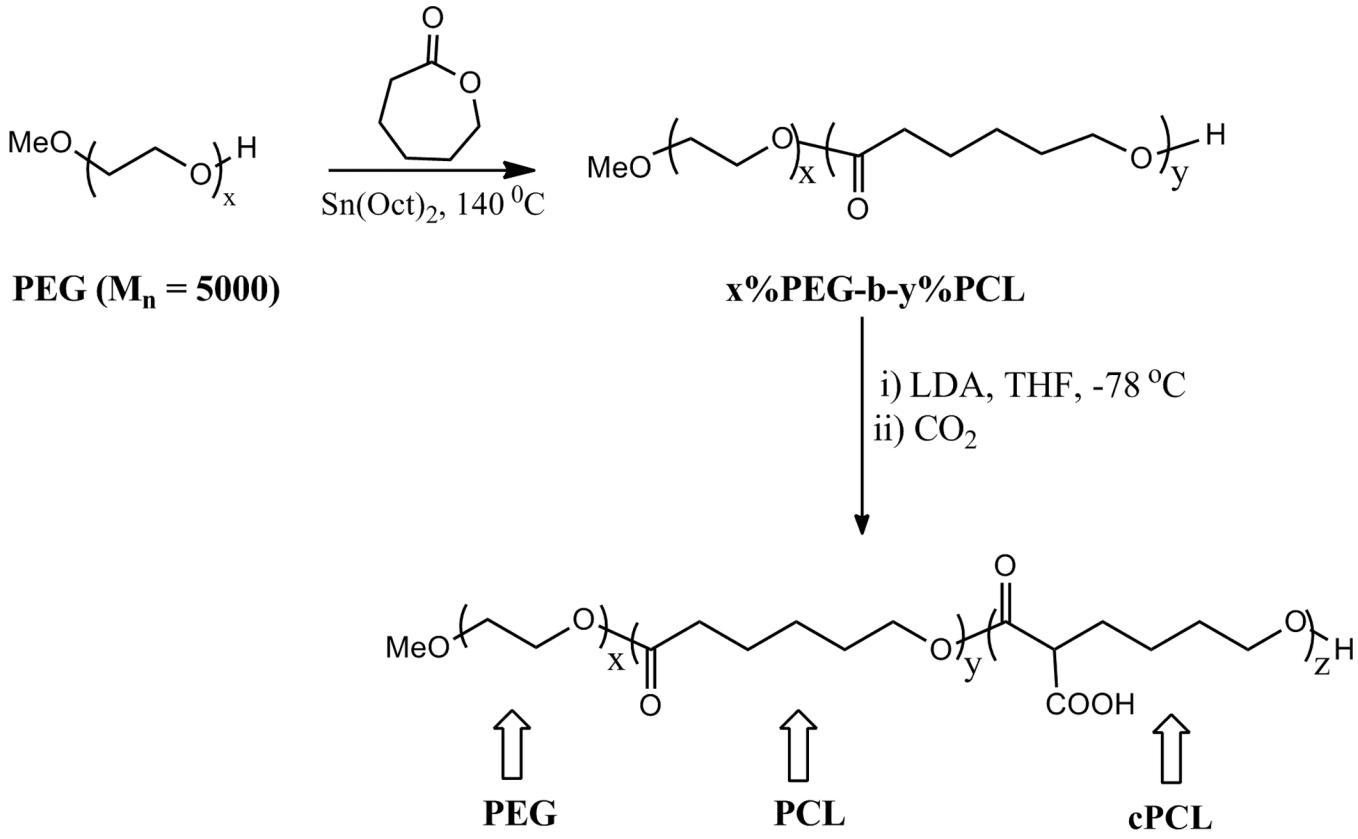

x%PEG-b-y%PCL-co-z%cPCL

B

Number-average molecular weight (M_n)

Polymer Composition	Day 0 (kDa)	Day 4 (kDa)	Day 7 (kDa)	Day 28 (kDa)	% M_n Remaining
100%PCL	93.2	86.9	84.1	80.7	86.6%
90%PCL-10%cPCL	139.1	135.7	133.2	112.4	80.8%
4%PEG-86%PCL-10%cPCL	95.3	92.2	85.7	71.3	74.8%

Figure 1. Polymers synthesis and degradation

(A) Schematic representation of polymer synthesis. The random copolymer is identified as x %PEG-b-y%PCL-co-z% cPCL where x, y, and z represent the respective molar ratio. PEG-PCL is a block copolymer, but the addition of cPCL is random within the PCL subunit. The polymers are abbreviated x%PEG-y%PCL-z%cPCL. **(B)** Degradation results for three representative polymers. Values were obtained by GPC using light scattering dn/dC measurements and represent the average of four M_n measurements. Percent remaining represents the M_n at day 28 relative to the initial value. These polymers were selected as representative samples in order to demonstrate how each subunit affects degradation properties.

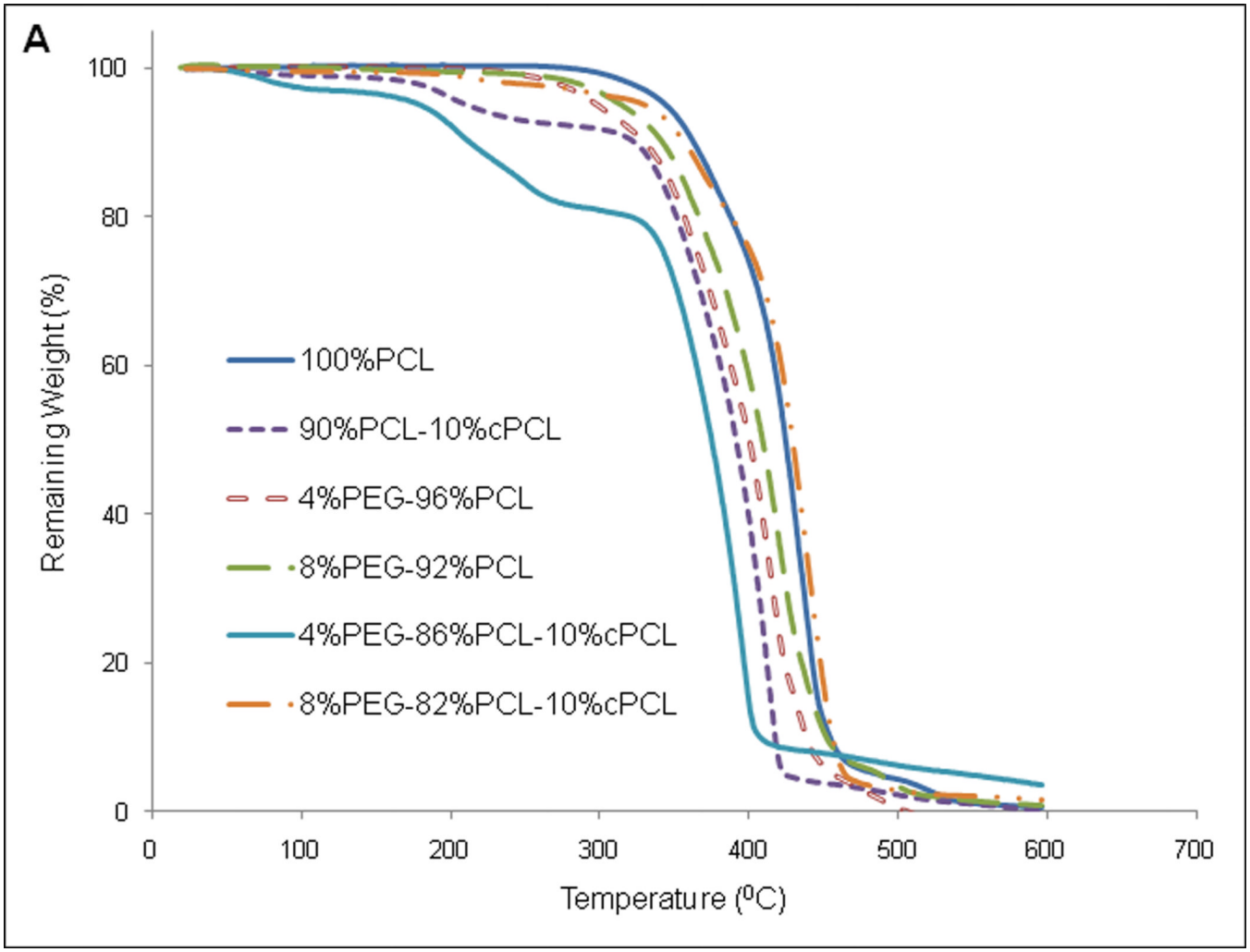

2B

Polymer Composition	ΔH (J/g)	T_m (°C)
100%PCL	79.2 ± 4.0	58.0
90%PCL-10%cPCL	73.7 ± 1.4	57.8
4%PEG-96%PCL	82.2 ± 2.3	57.3
8%PEG-92%PCL	91.3 ± 5.5	58.0
4%PEG-86%PCL-10%cPCL	58.1 ± 4.7	57.0
8%PEG-82%PCL-10%cPCL	71.0 ± 1.1	57.1
100%PEG	216.7 ± 4.3	60.5

Figure 2. Thermal properties of dry polymers

(A) Thermogravimetric analysis and **(B)** differential scanning calorimetry (DSC) of dry polymer samples. In part **(B)**, enthalpy change (ΔH) and melting temperature (T_m) were obtained from the second heating curve and represent the average of three measurements (n = 3). ΔH values are presented as average ± standard error of the mean.

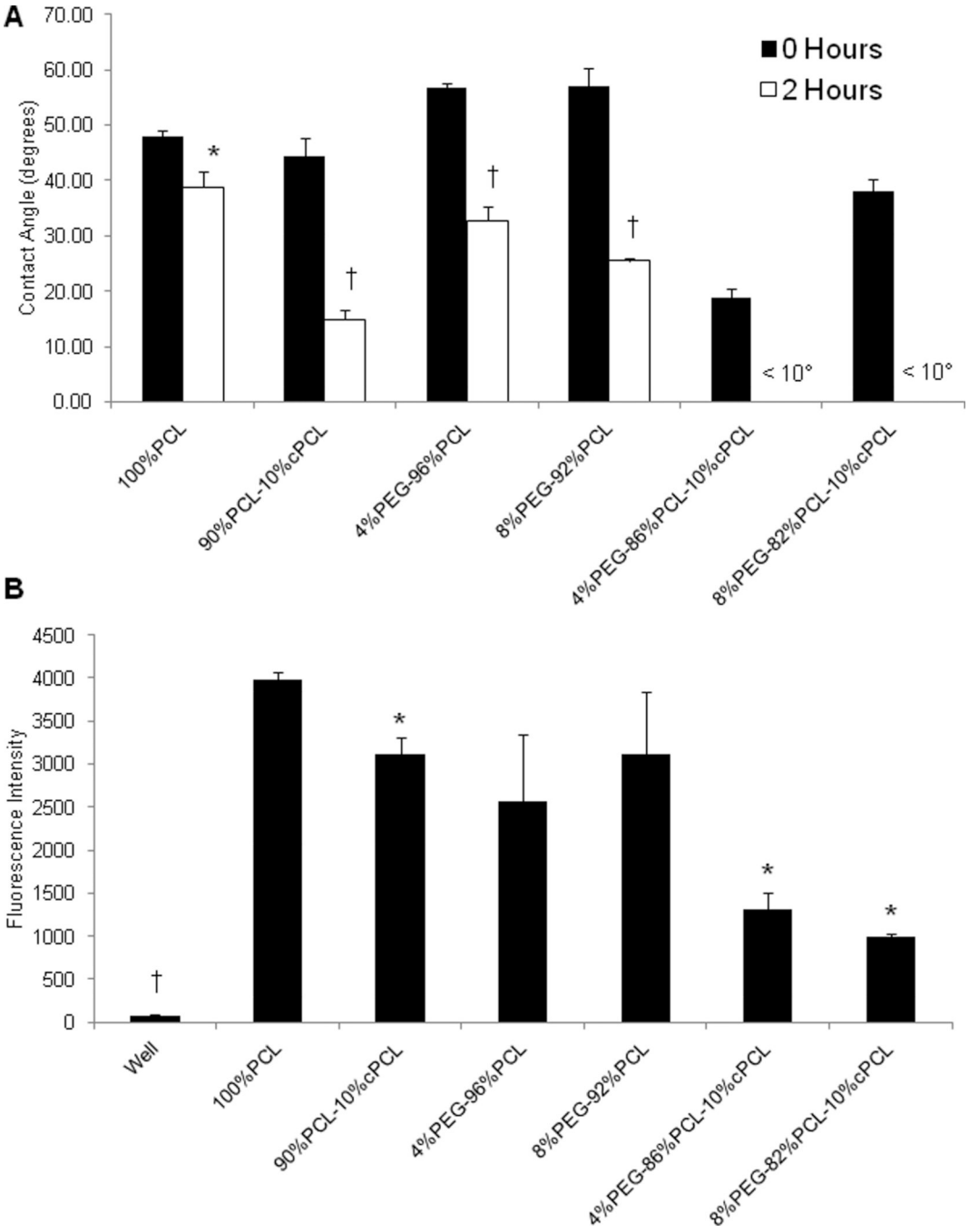

Figure 3. Surface chemistry

(A) Advancing contact angle analysis for polymer film surfaces (n = 3). Polymer samples were incubated with one drop of dH_2O for 2 hours at 37°C. At 2 hours for both 4%PEG-86%PCL-10%cPCL and 8%PEG-82%PCL-10%cPCL, contact angle value is < 10° because the drop was absorbed by the material. *$p < 0.05$, †$p < 0.01$ between 0 and 2 hours measurements on the sample polymer type. **(B)** Polymer-coated glass cover slips were incubated with carboxylate-terminated, fluorescence-conjugated polystyrene microspheres to evaluate surface chemistry. Negative surfaces exhibit a lower fluorescence signal, likely due to steric hinderance and/or charge repulsion (n = 4). *$p < 0.05$ *vs.* 100%PCL, †$p < 0.05$ *vs.* all other test substrates.

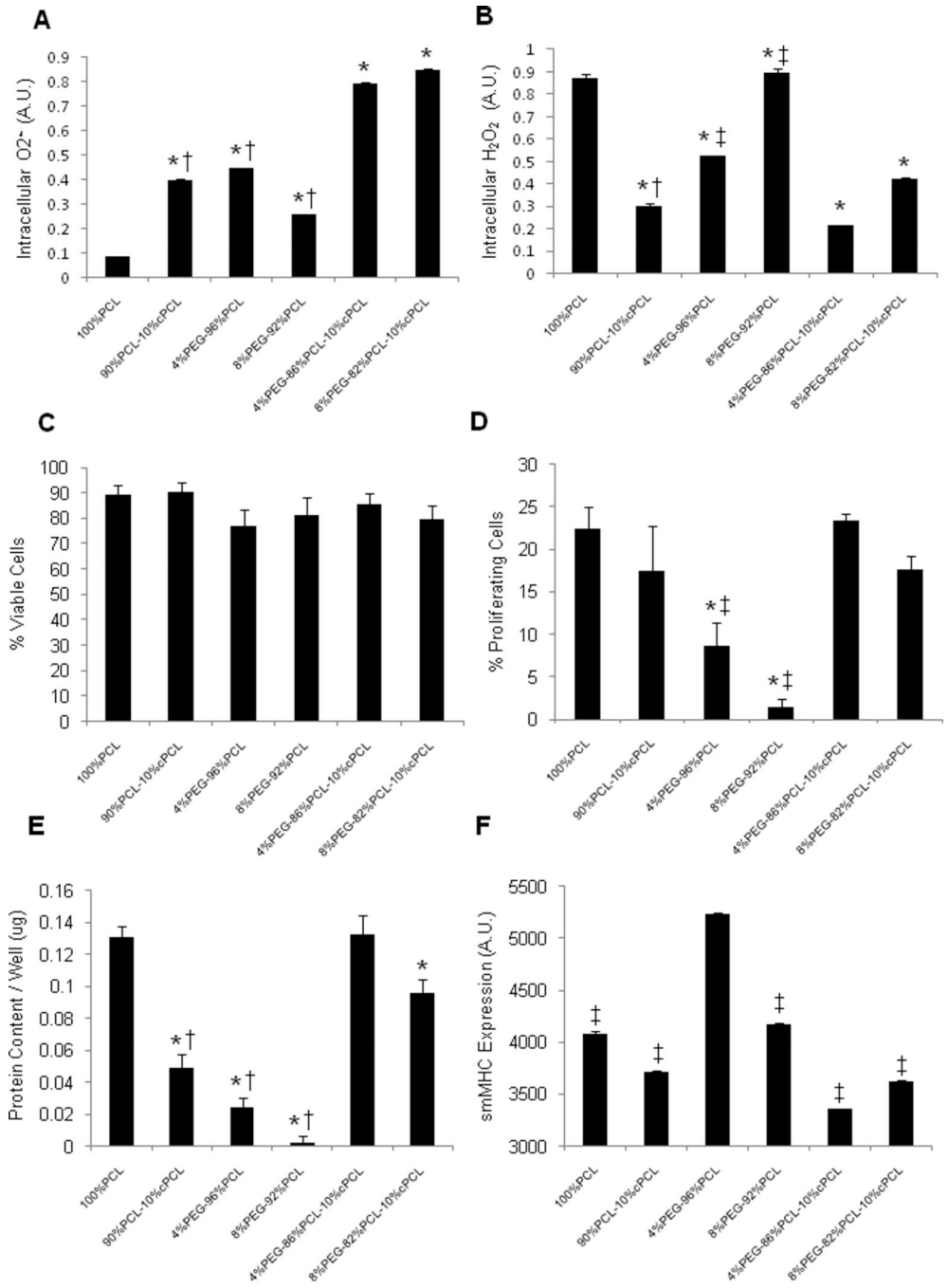

Figure 4. HCASMCs interaction with polymers

(A) Intracellular $O_2^{\bullet -}$ and **(B)** H_2O_2 measured by DHE and DCFDA, respectively (n = 3). **(C)** Cell viability and **(D)** percent proliferating HCASMCs as determined by calcein and BrdU staining, respectively (n = 6 – 12). **(E)** Total content of intracellular proteins and **(F)** smooth muscle myosin heavy chain (smMHC) expression (n = 16 – 30). All cellular interaction experiments were conducted at three days of culture on test polymer substrates. Statistical markers: **(A–E)** *$p < 0.01$ *vs.* 100%PCL; †$p < 0.05$ and ‡$p < 0.01$ *vs.* either test terpolymer. **(F)** ‡$p < 0.01$ *vs.* 4%PEG-96%PCL.

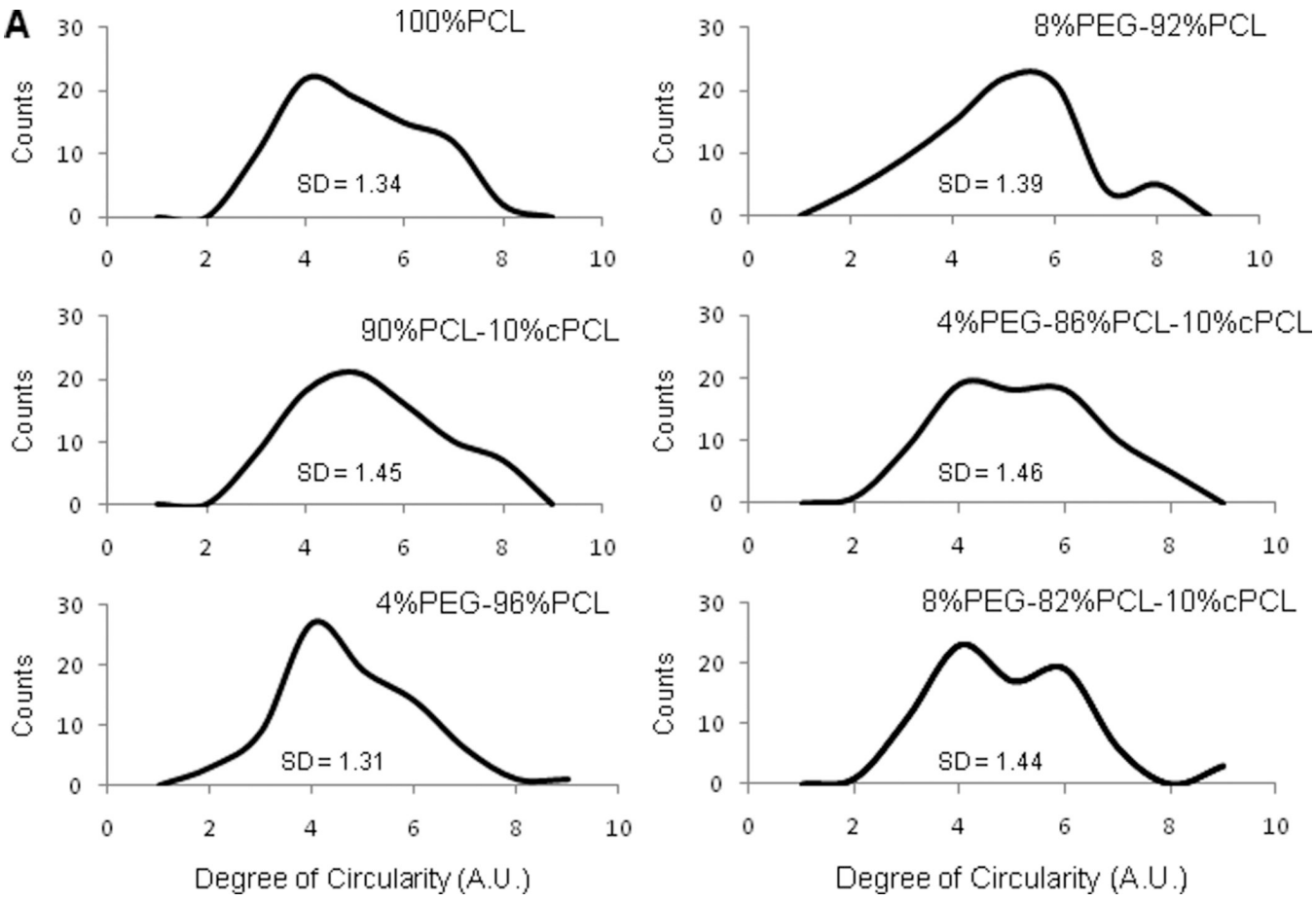

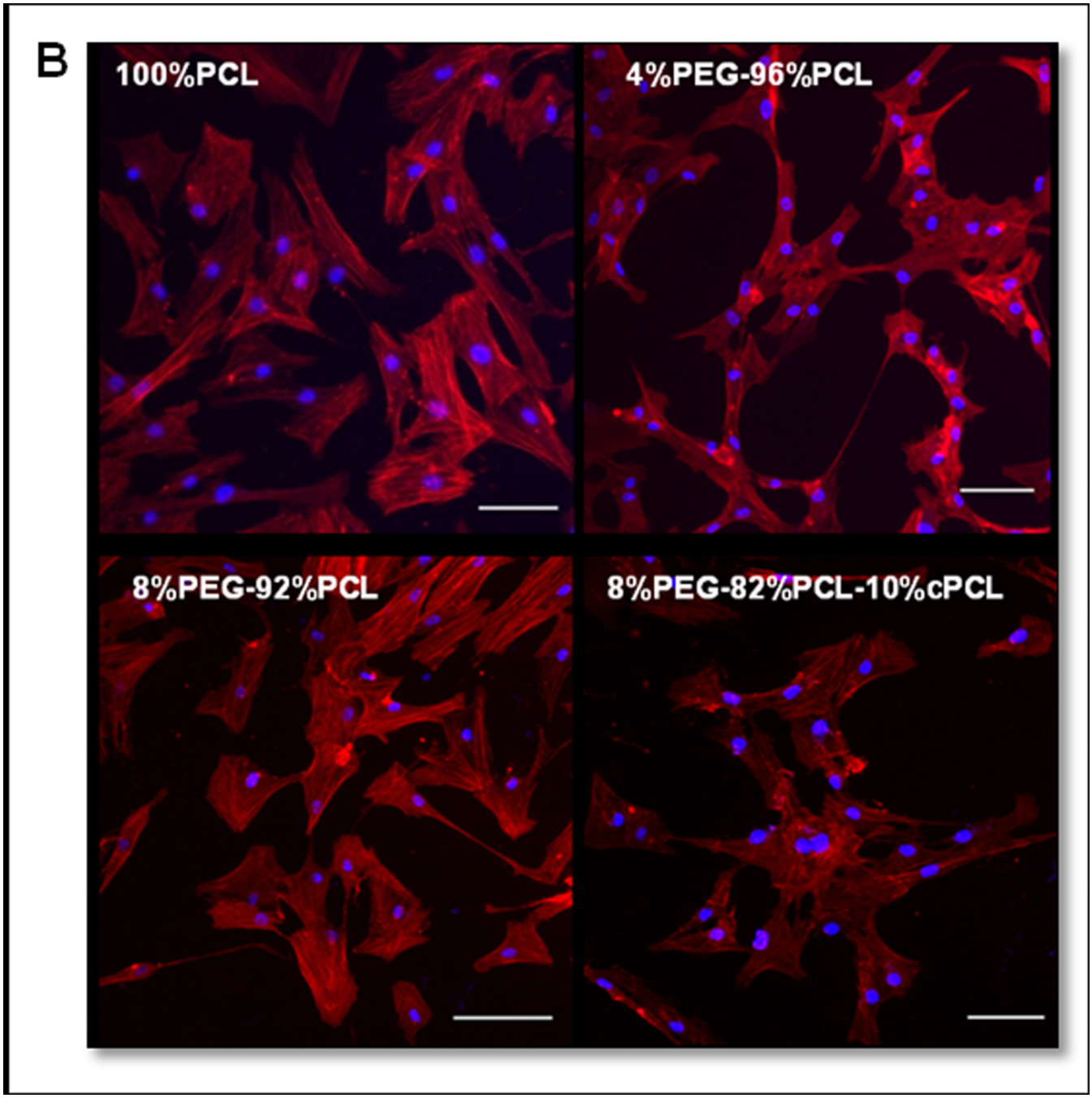

Figure 5. HCASMCs morphology

(A) Histograms of circularity distribution for HCASMCs grown on test substrates for three days (n = 80). Degree of circularity ranges from 0 (elongated) to 10 (perfect circle). SD = standard deviation of cell circularity for each polymer type. **(B)** Fluorescence images of HCASMCs stained with phalloidin (red) and Hoechst (blue) on four different polymer types. Scale bars = 100 μm.

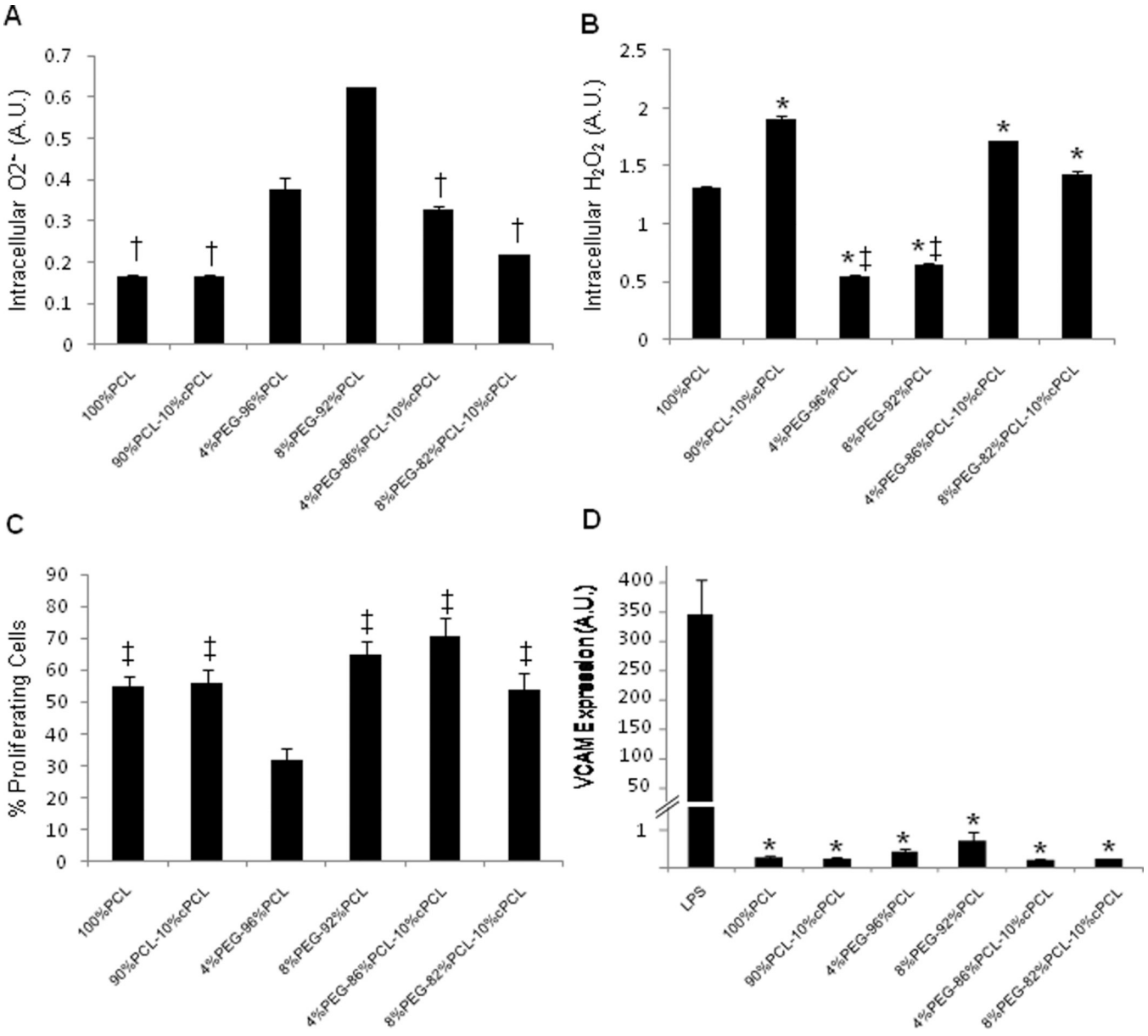

Figure 6. HCAECs interaction with polymers

(A) Intracellular $O2^{\bullet -}$ and **(B)** H_2O_2 measured by DHE and DCFDA, respectively (n = 3). **(C)** Percent proliferating HCAECs as determined by BrdU staining (n = 8 – 12). **(D)** Vascular cell adhesion molecule (VCAM) expression (n = 4). All cellular interaction experiments were conducted at three days of culture on test polymer substrates. Statistical markers: **(A)** †$p < 0.05$ *vs.* 8%PEG-92%PCL. **(B)** *$p < 0.01$ *vs.* 100%PCL, ‡$p < 0.01$ *vs.* either test terpolymer **(C)** ‡$p < 0.01$ *vs.* 4%PEG-96%PCL. **(D)** *$p < 0.01$ *vs.* LPS-treated control.

Table 1
Mechanical and thermal properties of wet polymers

Wet glass transition temperature (T_g), wet Young's modulus (E), and wet ultimate tensile stress (σ_U) were obtained with dynamic mechanical analysis (DMA) using solvent casted film samples incubated in dH_2O for two days at 37 °C.

Polymer Composition	Wet T_g (°C)	Wet E (MPa)	Wet σ_U (MPa)
100%PCL	−57.5	232.6 ± 49.6	14.6 ± 3.4
90%PCL-10%cPCL	−58.1	122.4 ± 49.4	7.0 ± 2.5
4%PEG-96%PCL	−57.9	145.6 ± 44.8	11.9 ± 3.3
8%PEG-92%PCL	−59.6	178.0 ± 47.3	13.0 ± 4.0
4%PEG-86%PCL-10%cPCL	−59.8	43.6 ± 2.9	2.4 ± 0.6
8%PEG-82%PCL-10%cPCL	−59.4	11.9 ± 4.1	0.6 ± 0.3